

ENHANCEMENT OF MAGNETOELECTRIC RESPONSE IN COMPOSITE BASED ON POLYVINYLIDENE FLUORIDE AND COBALT FERRITE SUSPENSION DUE TO NANOPARTICLE DISPERSION

© 2025 P. A. Vorontsov*, V. D. Salnikov, V. V. Savin, V. G. Kolesnikova,
P. A. Ershov, V. V. Rodionova

*Research Educational Center «Smart Materials and Biomedical Applications»,
Immanuel Kant Baltic Federal University, Kaliningrad, Russia*

Received November 15, 2024

Revised December 14, 2024

Accepted December 30, 2024

Abstract. We presented the results of the study of a nanocomposite of polyvinylidene fluoride and cobalt ferrite nanoparticles coated with oleic acid. It is found that the nanocomposite has low porosity and highly dispersed distribution of nanoparticles in the polymer matrix, due to which it exhibits a strong effect for polymer-based magnetoelectric composites - 24.5 mV/(cm-E). This makes the studied material promising for use in biomedical applications as a scaffold for cell stimulation.

Keywords: *polyvinylidene fluoride, cobalt ferrite, multiferroic, magnetoelectric*

DOI: 10.31857/S03676765250416e5

INTRODUCTION

The development of flexible functional magnetoelectric (FE) materials is interesting due to the possibility of their use in biomedicine [1, 2], sensorics [3, 4], electronics [5], and other fields. Hybrid multiferroic composite materials based on a

piezoelectric phase represented by a piezoelectric polymer and a ferromagnetic phase in the form of nano- and micro-filler deserve special attention. In this work, the piezoelectric polymer polyvinylidene fluoride (PVDF), which has a high piezoelectric modulus among polymers, and magnetic nanoparticles $\text{CoFe}_{(2)}\text{O}_4$, having high magnetostriction and saturation magnetization, were chosen as components of the ME composite. Such parameters of the composite components are necessary for the emergence of an enhanced direct ME effect in it, which is manifested in the polarization of the piezoelectric phase of the sample due to the transfer of mechanical stresses from the ferromagnetic phase, which changes its macro dimensions (magnetostriction effect) and tends to rotate and displace (nanoparticles in the external field) under the action of the external magnetic field [6]. Also due to biocompatibility and flexibility, ME composite based on PVDF and CoFe_2O_4 can be used in biomedical applications as scaffolds for cell stimulation [7-9].

Improving the distribution of magnetic nanoparticles (MNPs), i.e., increasing the dispersibility of the filler in the form of nanoparticles in the PVDF polymer matrix, is a promising approach to enhance the ME response [10]. Among the possible ways to realize such an approach is the use of coating the ferromagnetic filler with surface active substances (surfactants) - both to create stable colloidal solutions, which allows to create composites with a highly dispersed distribution of TPL in the polymer matrix, and to enhance the bonding between the components .[10]

The end groups of oleic acid (OA) have affinity to PVDF molecules, which leads to better dispersion of nanoparticles in the polymer matrix by reducing agglomeration and sedimentation of particles[11] , i.e., the OA layer on the surface of cobalt ferrite

interacts with the PVDF matrix through hydrophobic interactions[10] . In addition, the OC as a surfactant can act as an interface between a ferromagnetic and a segmentoelectric. Such interactions also improve the mechanical properties of the composite by reducing agglomeration [11,12] .

Thus, surface modification of $\text{CoFe}_{(2)}\text{O}_4$ nanoparticles with oleic acid can increase the ME coefficient. The study of the ME effect in composites based on polyvinylidene fluoride with a filler in the form of cobalt ferrite nanoparticles coated with OC is an urgent task for development of modern materials with improved multiferroic properties.

EXPERIMENTAL PART

Polyvinylidene fluoride manufactured by Sigma-Aldrich (m.m. 534,000) in the form of white powder, which was dissolved in N,N-Dimethylformamide (CHF), was used to fabricate the nanocomposite. $\text{FeCl}_3 \times 6\text{H}_2\text{O}$ (PDE), $\text{CoCl}_{(2)} \times 6\text{H}_{(2)}\text{O}$ (PDE), HCl (CHF), tetrahydrofuran (THF, dry), NaOH (PDE), and oleic acid were used to synthesize and modify the surface of the nanoparticles.

Synthesis of cobalt ferrite nanoparticles coated with oleic acid

To fabricate the nanoparticles, $\text{FeCl}_3 \times 6\text{H}_2\text{O}$ (0.004M) and $\text{CoCl}_{(2)} \times 6\text{H}_2\text{O}$ (0.002M) salts were used and dissolved in 12.5 mL of 0.04M hydrochloric acid and stirred at 80 °C. The solution was then added dropwise to 50 mL of sodium hydroxide (1M, 80 °C). To the resulting precipitate, 200 mL of water was added and the pH of the medium was adjusted to 7.4. The particles were re-precipitated by a permanent field

magnet, after which excess moisture was removed in a desiccator at 60 °C. After drying, the surface of the particles was modified with oleic acid in the presence of tetrahydrofuran [13,14] .

Creation of nanocomposite

CoFe₂O₄@OK/PVDF composite films were fabricated by the doctor blade method[15] . PVDF and the solvent dimethylformamide were taken in ratio of 1:4.8 and left to stir until homogeneous for 20 h. Into the dissolved polymer was added 1.43 mL of a suspension of CoFe₍₂₎O₄nanoparticles in THF, pre-dispersed in an ultrasonic bath (37 kHz), the concentration of MNF was 10% wt. %. The resulting mixture was stirred until homogeneity, after which the composite solution was uniformly spread with a doctor blade with a given thickness (50 μm) on an amorphous glass substrate. The obtained nanocomposite was placed in a desiccator at 65 °C for 20 h.

Structural characterization

X-ray diffraction analysis was performed on an AXRD PROTO benchtop powder X-ray diffractometer with Cu-Kα radiation source ($\lambda = 1.54056 \text{ \AA}$). The average coherent scattering area (D_{XRD}) was calculated using the Scherrer formula for the most intense peak:

$$D_{XRD} = \frac{0.94 \cdot \lambda}{\beta \cdot \cos\theta}, \quad (1)$$

where λ is the X-ray wavelength, β is the total width at half-height of the peak determined after fitting the peaks using the Voigt function, and Θ is the Bragg angle.

The lattice constant (a) for the cubic structure was calculated using the formula:

$$a = d \cdot \sqrt{h^2 + k^2 + l^2}, \quad (2)$$

where d is the interplanar distance, h, k and l are Miller indices ($h \cdot k \cdot l$)

The X-ray diffractogram for $\text{CoFe}_{(2)}\text{O}_4@\text{OK}/\text{PVDF}$ (Figure 1) consists of a set of reflexes that correspond to the XRD diffractogram of PVDF matrix and $\text{CoFe}_{(2)}\text{O}_4$ filler. The position of PVDF reflexes indicates the presence of several crystalline phases in the composite including α -, β - and γ -phases [16,17], which is consistent with literature data for nanocomposites fabricated by the doctor blade method [10].

According to the X-ray diffraction analysis, the crystal structure of the obtained MSNFs (Fig. 1) corresponds to cubic spinel [18]. The particle size calculated by the Scherrer method was ~ 3 nm. The lattice parameter of the synthesized cobalt ferrite MNFs was close to that of bulk cobalt ferrite $a = 8.41 \text{ \AA}$ [19]. It is worth noting that the halo appearing in the X-ray diffraction pattern for nanoparticles is caused by both the relatively high proportion of amorphous component and the small size of nanoparticles.

Topology and mechanical properties of the surface

A scanning electron microscope (SEM, Hitachi TM4000 Plus) in the electron backscattering mode was used to study the supramolecular structure of the nanocomposite and the distribution of MSNFs in the composite films.

The SEM images in Fig. 2 show the local structure of the composite surface. The bright areas correspond to the TPLs located on the polymer surface. Fig. 2a demonstrates that the TPLs are uniformly distributed throughout the entire volume of composite. In Fig. 2b, pores with the size of $1.6 \pm 0.4 \text{ \mu m}$ are marked in red color, large

agglomerates of $\text{CoFe}_{(2)}\text{O}_4@\text{OK}$ (3.5 ± 0.7 μm), which, in turn, consist of smaller agglomerates - 0.6 ± 0.1 μm (blue color), are highlighted in yellow. Due to coating of MWCNTs with oleic acid, the synthesized nanocomposite has better distribution of MWCNTs in the polymer matrix and smaller size of CoFe_2O_4 agglomerates , as compared to other works [20,21] . The nanocomposite fabricated by doctor blade method is characterized by the presence of pores, however, the fabricated material exhibits smaller pores and in lesser number as compared to its counterparts [15,22] .

Surface topology studies were performed with an atomic force microscope (Ntegra, NT-MDT) in semi-contact mode on a 50×50 $\mu\text{m}^{(2)}$ (1024×1024) area using an NS15 cantilever (NT-MDT). Fig. 3 shows the AFM image of the surface of the fabricated nanocomposite. A number of parameters were determined from this image: the surface layer pore area fraction was 4.5%; the average size of spherulites was 5.0 ± 0.6 μm ; the size of large particle agglomerates was no more than 3.0 μm , with an average of 2.4 ± 0.7 μm . Thus, the data obtained with the atomic force microscope agree with the data obtained with the scanning electron microscope and confirm the fact that modification of the MNF surface with oleic acid leads to better dispersion of particles and their homogeneous distribution in the polymer matrix than in the works [10,21] .

Magnetic properties

Magnetic measurements were performed using a vibrating magnetometer (VSM, Lakeshore 7400 System) in the field range up to 10 kE at room temperature (~295 K). Measurements of films with the size of 10×10 mm^2 were performed when an external magnetic field was applied in the sample plane.

Figure 4 shows the hysteresis loops for $\text{CoFe}_{(2)}\text{O}_4@\text{OK}$ nanoparticles (green line) and $\text{CoFe}_{(2)}\text{O}_4@\text{OK}/\text{PVDF}$ polymer composite (blue line). Both nanoparticles and composites are characterized by superparamagnetic behavior of the investigated systems. The coercivity of the samples was estimated from the hysteresis loops: $H_c = 10 \text{ \AA}$ for $\text{CoFe}_2\text{O}_4@\text{OK}$, $H_c = 60 \text{ \AA}$ for the composite. The increase in the coercive force is due to the fact that the presence of coating on the particles contributes to a better distribution of them in the matrix and the formation of smaller agglomerates, which leads to an increase in the dipole-dipole interaction between the particles within the agglomerates.

Magnetoelectric measurements

The longitudinal magnetoelectric effect of $\text{CoFe}_2\text{O}_4@\text{OK}/\text{PVDF}$ composite, in which the direction of the external magnetic field coincides with the polarization direction of the sample, was evaluated using the dynamic method .[23,24]

A sample of $10 \times 10 \text{ mm}^2$ was placed in an alternating magnetic field H_{AC} generated by Helmholtz coils with an amplitude of 1.5 E and frequency of 770 Hz, and a constant magnetic field H_{DC} varying in the range from 0 to 10 kE. The voltage V_{out} , generated at the sample surface, was detected using a lock-in SR 830 amplifier (Stanford Research Systems). The ME coefficient was calculated by the formula:

$$\alpha_{\text{ME}} = \frac{V_{out}}{t \cdot H_{AC}}, \quad (3)$$

where t is the thickness of the sample.

The field dependence of the longitudinal magnetoelectric coefficient, α_{ME} , on the magnitude of the constant magnetic field in the $\text{CoFe}_2\text{O}_4@\text{OK}/\text{PVDF}$ composite is

shown in Fig. 5. The dependence of the magnetoelectric coefficient on the applied constant magnetic field has a characteristic shape with the maximum value of the ME coefficient, $\alpha_{M\Theta} = 24.5 \text{ mV}/(\text{cm}\cdot\text{E})$, observed at a constant magnetic field value of 4 kE. This dependence is typical for polymer composites with ferromagnetic nanoscale filler: the external magnetic field, in which the maximum value of the ME coefficient is observed, is determined by the field of anisotropy of nanoscale particles[8] . The increase in the value of the ME coefficient obtained in the fabricated nanocomposite, compared to the value of 18 mV/cm-E obtained earlier [8], is achieved due to the better distribution of nanoparticles inside the polymer due to the modification of their surface with oleic acid.

CONCLUSION

Thus, we have performed a comprehensive structural and magnetic characterization of a composite based on piezoelectric polymer PVDF and cobalt ferrite MNF with a surface modified with oleic acid. X-ray diffraction analysis data confirmed the cubic spinel structure of the particles, and the particle size was determined to be $\sim 3 \text{ nm}$. Magnetic field measurements revealed a superparamagnetic response for both $\text{CoFe}_{(2)}\text{O}_4@\text{OK}$ and $\text{CoFe}_{(2)}\text{O}_4@\text{OK}/\text{PVDF}$ composites. Due to the modification of the surface of $\text{CoFe}_{(2)}\text{O}_4$ MWCNTs with oleic acid, a high degree of dispersion and the absence of large agglomerates of MWCNTs in the polymer matrix were achieved, which contributes to an increase in the efficiency of stress transfer between the magnetic and segmentoelectric phases and, consequently, to the improvement of the magnetoelectric characteristics of the composite: a high value of

the magnetoelectric coefficient for this type of material was obtained $-\alpha_{M\Theta} = 24.5$ mV/(cm-E).

The study demonstrated the significance of uniform distribution of $\text{CoFe}_{(2)}\text{O}_4$ nanoparticles inside PVDF piezopolymer for enhanced ME response. Polymer-based composites with enhanced ME effect are promising for their application as a framework for cell stimulation.

FUNDING

The study was financially supported by the Russian Science Foundation under Project No. 21-72-30032. The authors express their gratitude to the State Autonomous Institution KO OO SHILI, DPC (Kaliningrad) for providing the opportunity to conduct measurements on a scanning electron microscope and X-ray diffractometer.

REFERENCES

1. *Alibakhshi H., Esfahani H., Sharifi E.* // Ceram. Int. 2024. V. 50. No. 5. P. 8017.
2. *Subochev P.V., Orlova A.G., Turchin I.V. et al.* // Bull. Russ. Acad. Sci. Phys. 2018. V. 82. No. 5. P. 502.
3. *Behera C., Pradhan N., Das P.R., Choudhary R.N.P.* // J. Polym. Res. 2022. V. 29. No. 2. Art. No. 65.
4. *Shirinov A.V., Schomburg W.K.* // Sens. Actuators A. Phys. 2008. V. 142. No. 1. P. 48.
5. *Gheorghiu F., Stanculescu R., Curecheriu L. et al.* // J. Mater. Sci. 2020. V. 55. No. 9. P. 3926.
6. *Nan C.W., M. Bichurin, S. Dong et al.* // J. Appl. Phys. 2008. V. 103. No. 3. Art. No. 031101.
7. *Prasad P.D., Hemalatha J.* // Mater. Res. Express. 2019. V. 6. No. 9. Art. No. 094007.
8. *Omelyanchik A., Antipova V., Gritsenko C. et al.* // Nanomaterials. 2021. V. 11. No. 5. Art. No. 1154

9. Amirov A.A., Kaminskiy A.S., Arkhipova E.A. et al. // Bull. Russ. Acad. Sci. Phys. 2023. V. 87. No. 6. P. 715.

10. Botvin V., Fetisova A., Mukhortova Y. et al. // Polymers. 2023. V. 15. No. 14. Art. No. 3135.

11. Terzić I., Meereboer N.L., Mellema H.H., Loos K. et al. // J. Mater. Chem. C. 2019. V. 7. No. 4. P. 968.

12. Jovanović S., Spreitzer M., Tramšek M. et al. // J. Phys. Chem. C. 2014. V. 118. No. 25. P. 13844.

13. Zimina A., Nikitin A., Lvov V. et al. // J. Compos. Sci. 2024. V. 8. No. 2. Art. No. 48.

14. Botvin V.V., Shlapakova L.E., Mukhortova Y.R. et al. // Polymer (Guildf). 2024. V. 296. Art. No. 126765.

15. Savin V.V., Keruchenko M.A., Ershov P.A. et al. // Bull. Russ. Acad. Sci. Phys. 2024. V. 88. No. 4. P. 577.

16. Lei T., Cai X., Wang X. et al. // RSC Advances. 2013. V. 3. No. 47. P. 24952.

17. Mahato P.K., Seal A., Garain S., Sen S. // Mater. Sci. Pol. 2015. V. 33. No. 1. P. 157.

18. Nikishina E.E. // Fine Chem. Techn. 2022. V. 16. No. 6. P. 502.

19. Goldman A. Modem Ferrite Technology. Pittsburgh: Springer, 2006. 435 p.

20. Gao R., Chen C., Ren K. et al. // Mater. Today Chem. 2024. V. 42. Art. No. 102386.

21. Adhlakha N., Yadav KL. Truccato M. et al. // Eur. Polym. J. 2017. V. 91. P. 100.

22. Guillot-Ferriols M., Rodríguez-Hernández J.C., Correia D.M. et al. // Mater. Sci. Eng. C. 2020. V. 117. No. 117. Art. No. 111281.

23. Hassanpour Amiri M., Sharifi Dehsari H., Asadi K. // J. Appl. Phys. 2022. V. 132. No. 16. Art. No. 164102

24. Duong G. V., Grössinger R., Schoenhart M., et al. // J. Magn. Magn. Mater. 2007. V. 316. No. 2. Spec. Iss. P. 390.

FIGURE CAPTIONS

Figure 1. X-ray diffractograms for $\text{CoFe}_{(2)}\text{O}_4$ nanoparticles coated with oleic acid and $\text{CoFe}_{(2)}\text{O}_4@\text{OK}/\text{PVDF}$ composite.

Figure 2. SEM images of $\text{CoFe}_{(2)}\text{O}_4$ composite @OK/PVDF: general plan (a); enlarged area (b): pores (red), large agglomerates (yellow, small agglomerates (blue).

Figure 3. Surface topology of $\text{CoFe}_{(2)}\text{O}_4@\text{OK}/\text{PVDF}$ nanocomposite obtained by AFM.

Fig. 4. Dependence of magnetization on the applied external magnetic field for nanoparticles (green color) and composites with nanoparticles (blue color).

Figure 5. Field dependence of the magnitude of the longitudinal ME coefficient of the $\text{CoFe}_{(2)}\text{O}_4@\text{OK}/\text{PVDF}$ nanocomposite on the external constant magnetic field.

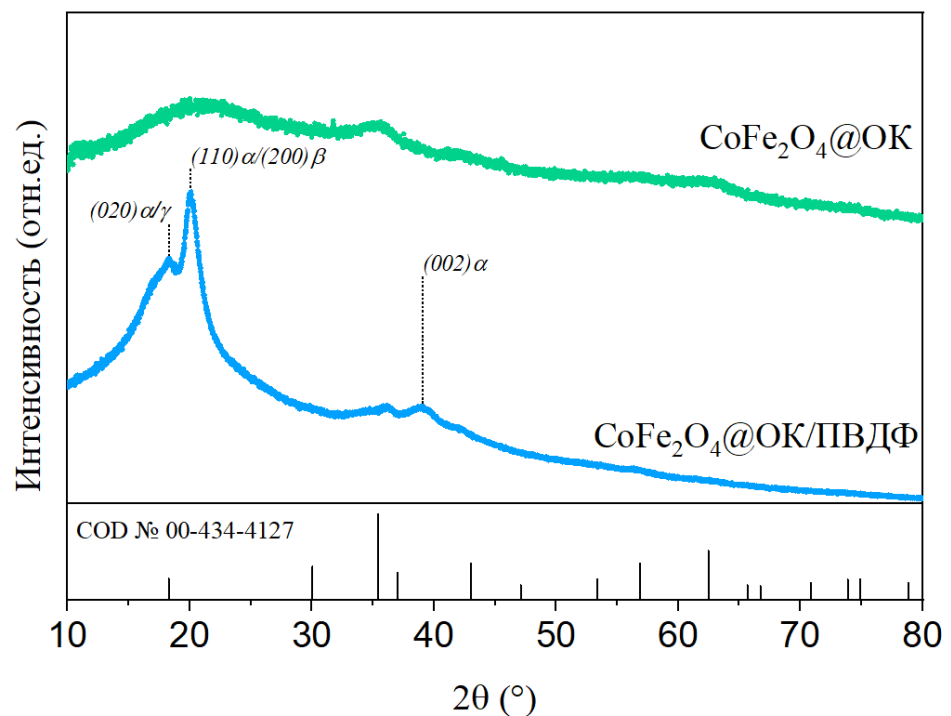


Fig. 1.

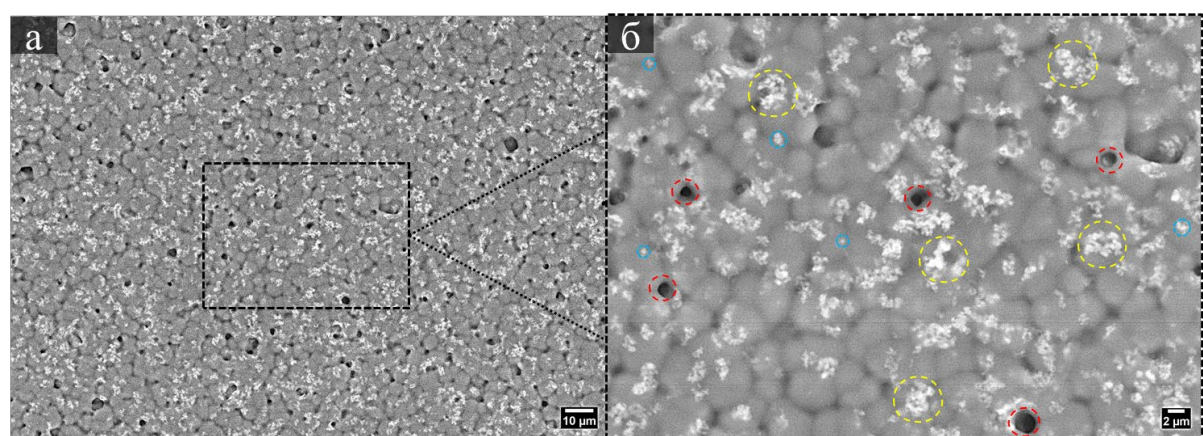


Fig. 2

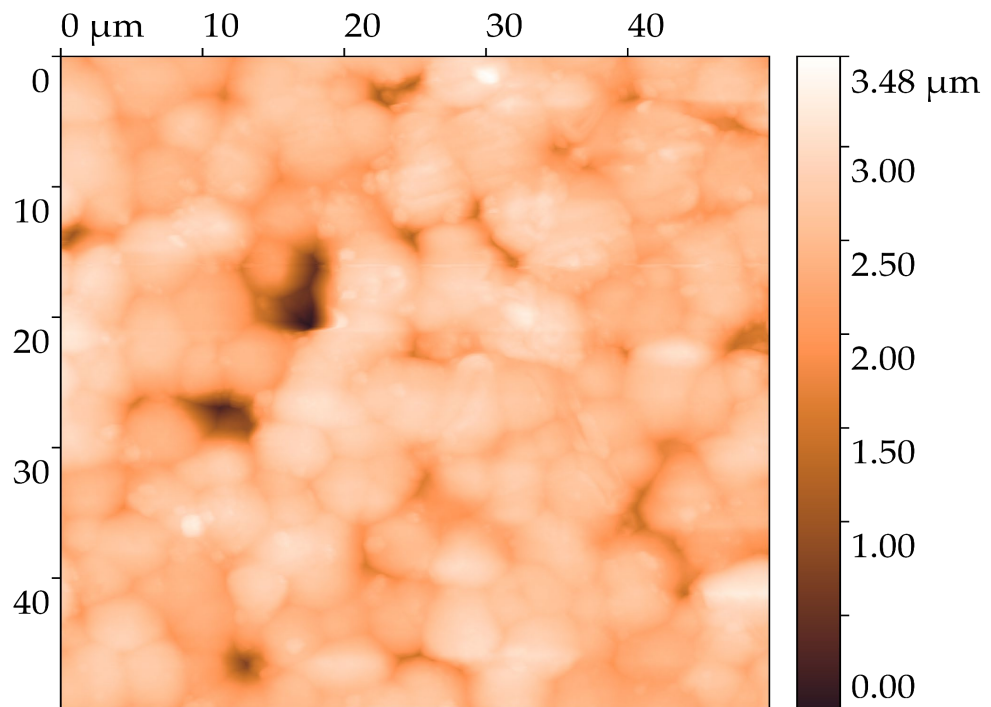


Fig. 3

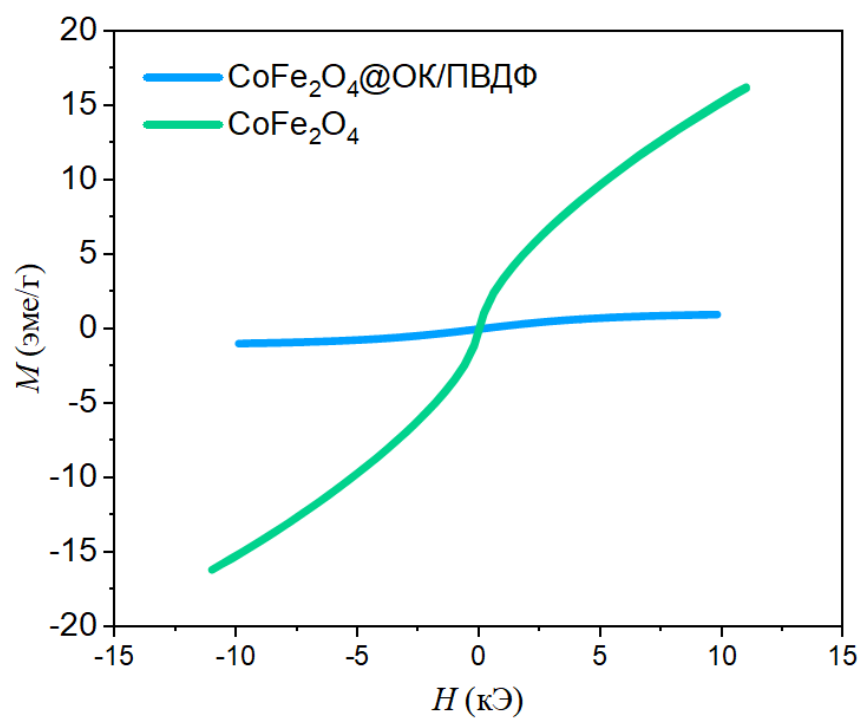


Fig. 4

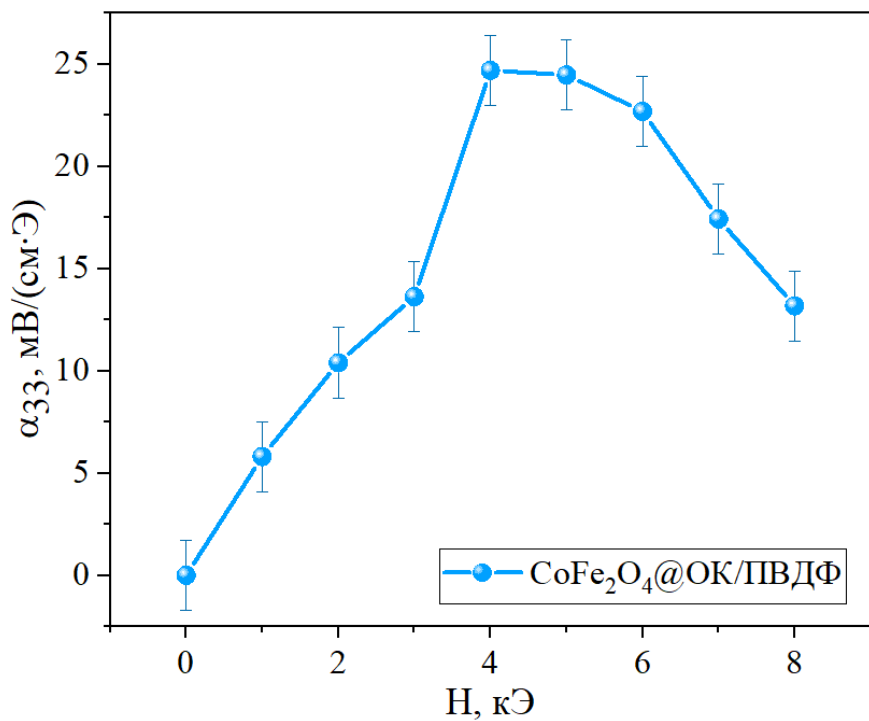


Fig. 5